Tunable Molecular Plasmons in Polycyclic Aromatic Hydrocarbons

Alejandro Manjavacas,[†] Federico Marchesin,[‡] Sukosin Thongrattanasiri,[†] Peter Koval,[‡] Peter Nordlander,[¶] Daniel Sánchez-Portal,[‡] and F. Javier García de Abajo[†,*]

[†]IQFR—CSIC, Serrano 119, 28006 Madrid, Spain, [‡]Centro de Física de Materiales CFM/MPC (CSIC-UPV/EHU) and Donostia International Physics Center (DIPC), Paseo Manuel de Lardizabal 4-5, 20018 San Sebastián, Spain, and [¶]Department of Physics and Astronomy, M.S. 61, Rice University, Houston, Texas 77005-1892, United States

ABSTRACT We show that chemically synthesized polycyclic aromatic hydrocarbons (PAHs) exhibit molecular plasmon resonances that are remarkably sensitive to the net charge state of the molecule and the atomic structure of the edges. These molecules can be regarded as nanometer-sized forms of graphene, from which they inherit their high electrical tunability. Specifically, the addition or removal of a single electron switches on/off these molecular plasmons. Our first-principles time-dependent density-functional theory (TDDFT) calculations are in good agreement with a simpler tight-binding approach that can be easily extended to much larger systems. These fundamental insights enable the development of novel plasmonic devices based upon chemically available molecules, which, unlike colloidal or lithographic nanostructures, are free from structural imperfections. We further show a strong interaction between plasmons in neighboring molecules, quantified in significant energy shifts and field enhancement, and enabling molecular-based plasmonic designs. Our findings suggest new paradigms for electro-optical modulation and switching, single-electron detection, and sensing using individual molecules.

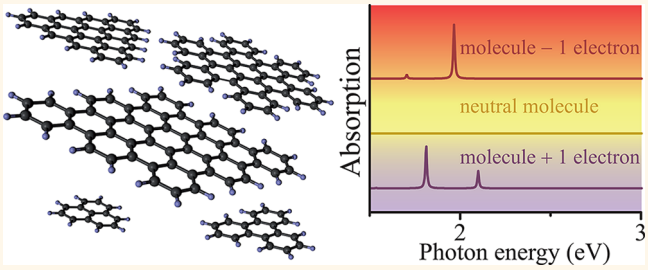

KEYWORDS: plasmonics · polycyclic aromatic hydrocarbons · molecular plasmonics · graphene plasmons · nanophotonics · TDDFT · tight-binding · RPA

Plasmonics has emerged as a promising path toward nanoscale light circuitry[1,2] and optical integration,[3,4] providing significant subwavelength confinement[5] and mechanisms for both spectral and spatial control over light propagation.[1,6,7] The remarkable structural tunability of plasmon resonances, as manifested from their strong dependence on size, composition, and shape of the supporting nanostructure,[8] enables light manipulation at the nanoscale, but demands exquisite fabrication accuracy.

Traditional plasmonic materials are simple and noble metals, which are molded into desired geometries by either chemical or lithographic methods. A vast amount of work has been devoted to producing monodispersive colloids of nanoparticles of these materials with specific morphologies such as spheres, shells, rods, stars, and simple polyhedra.[9] Integration of such nanoparticles into plasmonic systems using chemical self-assembly[10] offers a scalable strategy for high-yield synthesis of complex plasmonic nanostructures, although control over individual particle positions and interparticle gaps is generally poor and severely hampers the performance of the whole system. The alternative approach, based on lithography, provides better control over the relative positions of individual components, but suffers from limited spatial resolution ~10 nm and contamination from resists in electron and optical lithographies and from spurious atomic species in focused ion-beam milling.

In this article, we demonstrate plasmonic behavior (*i.e.*, genuinely collective electron oscillations) in a radically different type of materials, individual polycyclic aromatic hydrocarbons (PAHs). Specifically, we predict highly tunable low-energy plasmonic resonances in PAHs using time-dependent density-functional theory (TDDFT, see Methods). These molecules, which consist of finite arrangements of aromatic benzene rings and bear a close resemblance to the so-called graphene quantum dots,[11] are readily available through chemical synthesis[12−16] and have been extensively investigated in a variety of applications ranging from possible candidates for primitive forms of life[17] to device materials in electronic and optical applications.[13] While the electronic excitations and fluorescence properties of PAHs

* Address correspondence to J.G.deAbajo@nanophotonics.es.

Received for review February 5, 2013 and accepted March 13, 2013.

Published online March 13, 2013
10.1021/nn4006297

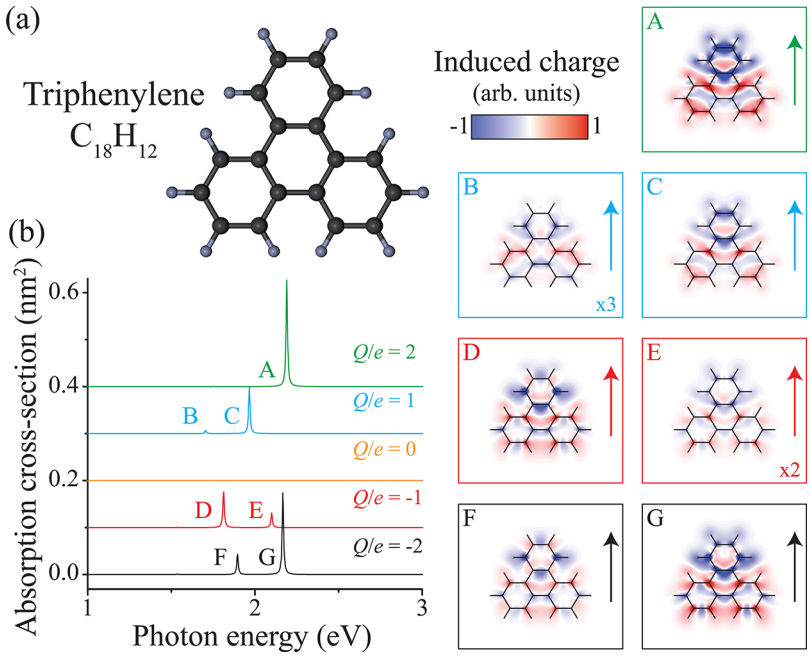

Figure 1. Plasmons in a small molecule: triphenylene. (a) Atomic structure of triphenylene. (b) Absorption cross-section spectra for different net charges *Q* of the molecule in units of the elementary charge *e*. The right panels show the induced charge density distributions (only the imaginary part, corresponding to real transitions at the selected frequencies) associated with the modes labeled in panel b. The incident electric field is along the direction of the arrows.

are well studied and understood,[18−20] their collective low-energy resonances and their dependence on the charge state and edge configuration have, to our knowledge, not been addressed previously. Using state-of-the-art theoretical calculations, we show the existence of pronounced collective electronic excitations in small systems consisting of less than 100 carbon atoms, and we find their frequencies to be strongly dependent on the charge state of the molecules. This behavior is reminiscent of the plasmons recently observed in doped graphene.[21,22] Furthermore, both the frequencies and the strengths of these resonances are strongly renormalized with respect to the one-electron transitions obtained in a noninteracting picture. For these reasons, in what follows we refer to these excitations as molecular plasmons. Interestingly, given the small size of the PAHs here studied, and in marked contrast to conventional metal-based plasmonics, molecular plasmons have a distinct quantum-mechanical origin, and cannot be described classically.

While the existence of plasmons has been extensively demonstrated in atomic-scale systems such as atomic chains,[23] fullerenes,[24] and carbon nanotubes,[25] we find that the PAH structures provide a more general strategy for nanoscale plasmonics because their molecular plasmons exhibit an exceptional structural and electrical tunability, as we show below. Just like graphene,[21,22,26] these carbon-based planar structures sustain plasmons that can be switched on/off through electrical doping. However, we find that the electrical tunability of PAHs is even greater than for graphene. Quite remarkably, we find that the plasmonic behavior of PAHs can be controlled by the addition or removal of a single electron. For comparison, raising the Fermi level of an individual sheet of graphene by 1 eV, which is an affordable change, requires adding one electron for every 50 carbon atoms, and thus, adding or removing one electron can be simply achieved through electrical gating in molecules of that size. A significant advantage with PAHs over graphene is that their extreme electrical tunability extends through the visible range of the spectrum, thus emphasizing their potential importance for optoelectronic technologies. As TDDFT becomes impractical for systems containing a large number of electrons, we here demonstrate that a tight-binding random-phase-approximation (TB-RPA) model[27] (see Methods) provides a fast, semiquantitative alternative for simulating the electronic and optical properties of large PAHs. This analysis can be straightforwardly extended to very large and coupled systems, in which PAHs can act as tunable integrated plasmonic components.

RESULTS AND DISCUSSION

Collective Electron Modes in Small PAHs. As a first example of a tunable plasmonic PAH, we analyze the optical properties of thiphenylene in Figure 1. This molecule consists of 18 carbon atoms arranged in three benzene rings. Like the rest of the molecules here considered, the carbon atoms along the edges are bound to hydrogen atoms (12 of them in this case). In its neutral form (charge state $Q = 0$), no observable excitation resonances are apparent in the 1−3 eV spectral range (Figure 1b), in agreement with the measured >4 eV absorption gap.[16] However, when an electron is either added or subtracted

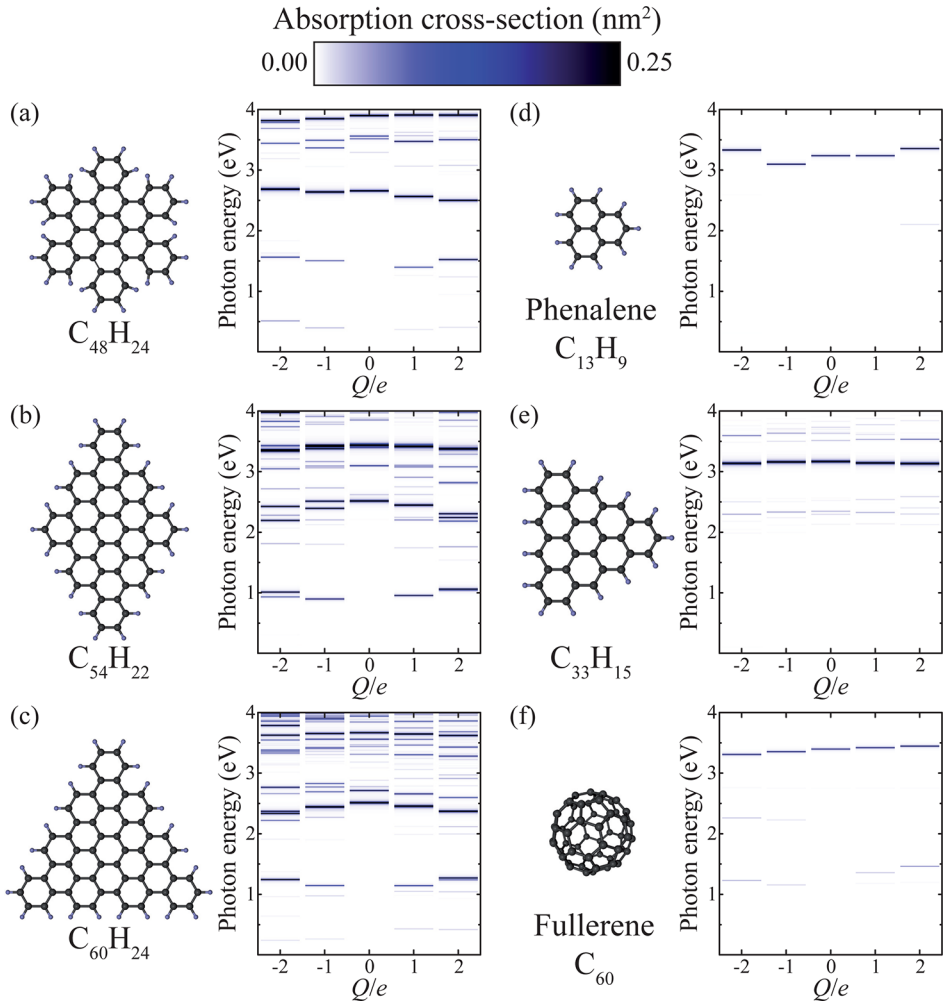

Figure 2. Molecular plasmonic zoo of polycyclic aromatic hydrocarbons (PAHs). (a–f) Atomic structure (left) and absorption spectra (right) for different sizes, shapes, and net charges. Fullerene is also analyzed for comparison (f). The spectra are given as absorption lines, in color scale saturated to 0.25 nm^2, so that saturated peaks have a thickness proportional to their absorption intensity. The incident field is along the vertical direction.

from the molecule, new strong features emerge in the absorption spectrum (slightly below 2 eV). A charge distribution analysis reveals that these modes have a strong dipolar character (see B–E panels in Figure 1), similar to those typically observed in coupled plasmonic systems, and support our identification of the absorption features in this PAH as molecular plasmons. A satellite peak is also discernible to the right (left) of the dominant feature for single electron (hole) doping. In the TB-RPA results, this satellite peak is much weaker and cannot be seen in the graph (see below). Adding a second electron or hole to the molecule results in an increased plasmon strength and a blue shift in energy, as expected from the higher concentration of doping charges.[28]

In Figure 2 we compare plasmons displayed by several different PAH molecules. The C_{60} molecule is also examined for comparison. By regarding these PAHs as fragments of graphene, we can classify them according to the difference between the number of atoms in each of the two carbon sublattices. This number difference gives rise to an equal number of electronic states at the Fermi energy of the neutral molecules[29] (here set to zero energy). These electronic states are localized along the atomic edges in large molecules, and thus, they can be identified as edge states. The presence or absence of these states have dramatic effects on the electronic structure[30] and also on the optical response of the molecules.[27] In particular, PAHs with armchair edges (Figure 2a–c) possess no zero-energy states, and therefore, there is a substantial HOMO–LUMO gap (*e.g.*, > 3 eV in triphenylene, see Figure 3b), which prevents the existence of low-energy electron–hole pair transitions, and also averts the possibility of having low-energy plasmons in the neutral molecule. However, the addition of an electron to the LUMO (or a hole to the HOMO) triggers new low-energy transitions, which interact collectively forming molecular plasmons. The mere existence and tunability of these plasmons is thus intimately linked to the absence of the noted zero-energy states. The excitation of these modes produces strong, distinct absorption features characteristic of dipolar plasmons. In particular,

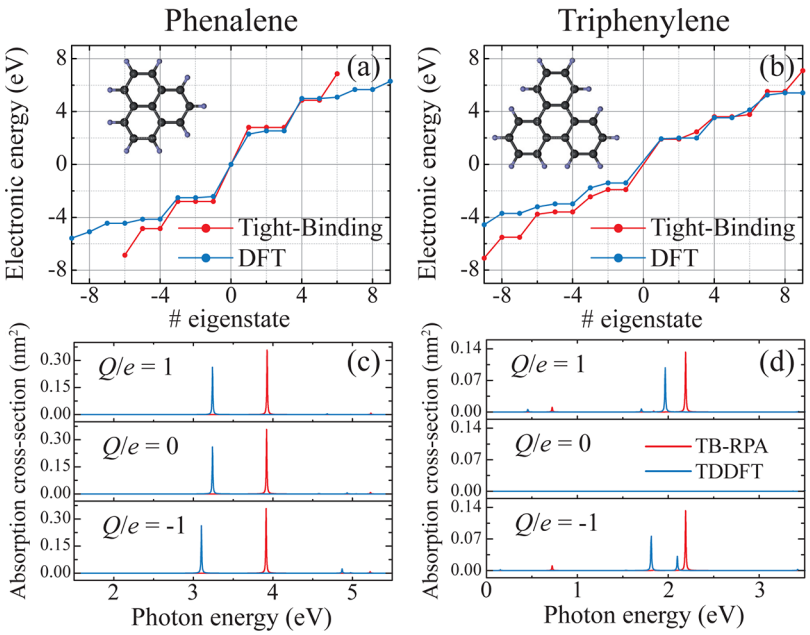

Figure 3. Toward a simple quantum-mechanical description of molecular plasmons. Comparison of electronic (upper panels) and optical (lower panels) properties calculated using TB-RPA (red) and TDDFT (blue) for (a,c) phenalene and (b,d) triphenylene with different net charges $Q/e = 0, \pm 1$.

low-energy plasmon bands emerge at energies below 2 eV in the armchair molecules considered in Figure 2a–c. These plasmons exhibit redshifts with increasing number of atoms and, like in thiphenylene (Figure 1), they undergo blue shifts with increasing charge state $|Q|$. This behavior is analogous to the frequency scaling $\omega \propto Q^{1/4}/N_a^{1/2}$ for plasmons in larger graphene nanostructures composed of N_a carbon atoms, as predicted from a classical electromagnetic description of the carbon layer when the geometrical shape is maintained,[31] in agreement with experimental observations.[21,22] However, the detailed dependence on Q and N_a in PAHs is severely corrected by quantum effects with respect to this classical scaling law. In particular, we find that the higher-energy plasmon bands in these molecules are also tunable with charge Q, but that in contrast to the low-energy band, their frequencies decrease with increasing $|Q|$ in some cases, which is a clear departure from the prediction of the above classical scaling law. The strong electron–hole symmetry of the electronic spectrum in PAHs explains why the energies of these plasmons are weakly dependent on the sign of the doping. Incidentally, similar charge-tunable, well-defined, low-energy plasmons are predicted in C_{60} (Figure 2f), as this molecule is equally free from zero-energy electronic states, although it does not have the noted electron–hole symmetry (see Supporting Information, SI).

In contrast to armchair PAHs, molecules with zigzag edges (Figure 2d,e) possess zero-energy electron states (*i.e.*, they have a *metallic* character, with partially filled states at the Fermi level), and therefore, the addition of one electron or hole does not substantially change the optical response because it does not open new electronic transitions. Only higher-energy plasmon bands (>2 eV) are observed in zigzag molecules, which are also present in armchair molecules and exhibit a relatively weak dependence on Q. Incidentally, zero-energy states contribute to the optical response by introducing additional electron–hole pair excitations that can quench the plasmons, and this can be an important effect in larger molecules, which involve smaller separations between electronic energy levels.[27]

Toward a Simplified Tight-Binding Description of Molecular Plasmons. Our finding of highly tunable plasmons in PAHs suggests that these molecules/materials may play an important role in existing and emerging plasmonic applications. A central theme in such applications is the coupling between individual plasmonic components resulting in larger integrated components. While the optical properties of small PAHs can be calculated using the first-principles TDDFT formalism, which includes a self-consistent description of all four carbon valence electrons (see Methods), this method cannot be extended to large finite systems. An accurate treatment of the largest PAHs investigated in Figure 2 already represents a sizable computational problem. For PAH-based plasmonics to become a practical reality, it is therefore essential to develop a more computationally efficient algorithm.

In Figure 3 we compare results from the TDDFT approach with results from the much simpler TB-RPA description, which can be carried out for nanostructures consisting of up to tens of thousands of atoms.[27] Remarkably, even for the smallest PAHs under consideration (Figure 3), TB-RPA also predicts the existence and absence of charge-tunable plasmons in triphenylene and phenalene, respectively. Similar quantitative

agreement regarding the charge tunability of PAHs is also obtained for larger molecules (see Supporting Information). However, the plasmon energies obtained from TB-RPA are consistently blue-shifted compared with the values obtained from TDDFT. This is due to the neglect of the σ electrons and the use of only one p_z orbital to represent each carbon site in TB-RPA. While the localized σ electrons do not contribute charges to the delocalized electrons that make up the plasmon, they introduce charge screening through their polarization (just like the d-electrons in noble metals[32]). Another difference between the two approaches is that TDDFT predicts slightly weaker absorption intensity for the plasmons. This could arise from hybridization among the larger number of basis set orbitals used in DFT (see Methods), thus possibly transferring oscillator strength from the low-energy π plasmons to higher-energy absorption bands. Despite these details, the overall agreement between TDDFT and TB-RPA is excellent and shows that TB-RPA provides a semiquantitative approach for the design and description of integrated PAH plasmonics.[27]

Effect of Self-Consistent Screening and the Nature of Molecular Plasmons. The small size of the PAHs under consideration raises the question of how many valence electrons are necessary to sustain well-defined plasmons? This issue is directly related to the understanding of plasmons as collective electron modes. In a recent report, it has been shown that plasmons can be separated from single-particle excitations because they are more sensitive to electron−electron interactions.[33] Here, we examine the role of electron−electron interactions at the self-consistent RPA level, which is shown to be crucial in determining the plasmon energies and their tunability (see below). We obtain analogous results from the TDDFT method (see Supporting Information), which includes the effects of electronic exchange and correlation within the local-density approximation.

Self-consistent screening is included in the TB-RPA method through the relation $\chi = \chi_0 \cdot (1 - v \cdot \chi_0)^{-1}$, where χ_0 is the RPA susceptibility,[34] χ is the full susceptibility, and v denotes the bare Coulomb interaction (see ref 27 for more details). The induced density is then obtained from the external potential as $\rho = \chi \cdot \phi^{ext}$. We have explored the role of self-consistent screening by comparing the results of this method with a modified version in which χ is replaced by χ_0 (*i.e.*, by removing the self-consistency in the Coulomb interaction among induced charges). The resulting spectra are plotted in Figure 4 for the smallest molecules under consideration. The energies of the plasmons (Figure 4a,b), which can be understood as involving collective electron motion driven by self-consistent Coulomb interaction among different electron−hole pair transitions, are radically different from the absorption features in the absence of that interaction (Figure 4c,d). The latter correspond to bare electron−hole pair transitions. This clearly shows that self-consistent screening is crucial

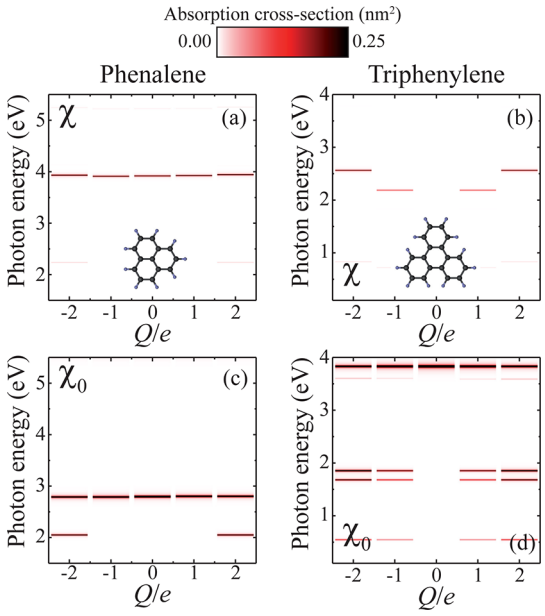

Figure 4. Effect of self-consistent screening on the optical response. (a,b) Absorption spectra of phenalene and triphenylene, obtained with the TB-RPA method, including self-consistent screening (default). (c,d) Spectra obtained by using χ_0 instead of χ, that is, by neglecting self-consistent screening.

to quantitatively predict plasmon energies in PAHs and indicates that our molecular plasmons are indeed collective oscillations that involve strong interaction between individual electron−hole pair excitations.

Plasmons in Linear Benzene Chains (Polyacenes). We examine the special class of PAHs that are composed of successively concatenated benzene rings as an atomic-scale version of plasmonic nanoantennas. The electronic properties of these molecules, also known as polyacenes, have been explored for a long time.[12,35,36] Although their edges are zigzag, they possess the same number of atoms in both carbon sublattices, and therefore, a gap between occupied and unoccupied states is present when they are uncharged. We thus expect similar tunability with the charge state as found for the PAHs considered above. A low-energy dipolar plasmon emerges in the charged molecules at low energies, as shown in Figure 5b (solid curves). This plasmon shifts to higher energy when the charge state increases from Q/e = 1 to 2. The second absorption feature is rather independent of charge state (Figure 5b, dashed curves). In all cases, similar to what happens with metallic nanoantennas, the plasmon energy shifts to lower values with increasing length of the molecule. In particular, the low-energy tunable feature occurs at a light wavelength that scales almost linearly with the number of benzene rings N (*i.e.*, similar to the approximate proportionality between the length and the dipolar plasmon wavelength in gold nanorods[37]). This is in contrast to the higher-energy feature, which saturates as N increases. The strength of the plasmon in the spectra also shows a striking difference in both cases: the

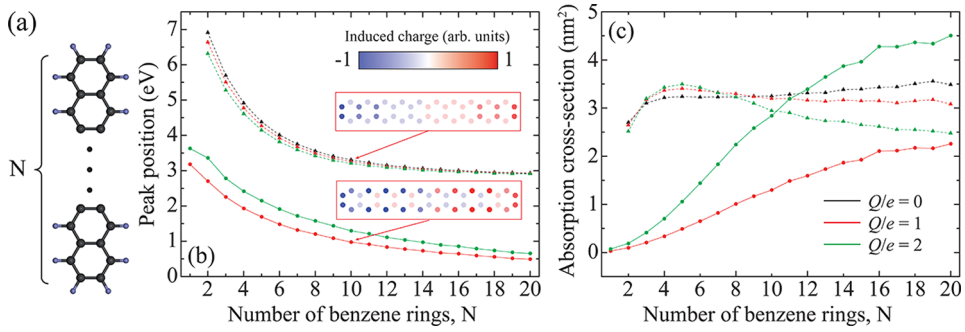

Figure 5. Tunable plasmons in linear benzene chains (polyacenes). We show the energy (b) and maximum extinction cross-section (c) associated with the plasmons of lowest and second-lowest energies in polyacenes as a function of the number of benzene cycles *N*, calculated with the TB-RPA method. Three different charge states are considered: *Q*/*e* = 0,1,2. The incident field is along the chains. Atom-resolved induced-charge distributions are shown in panel b as insets for *Q*/*e* = 1 and *N* = 10.

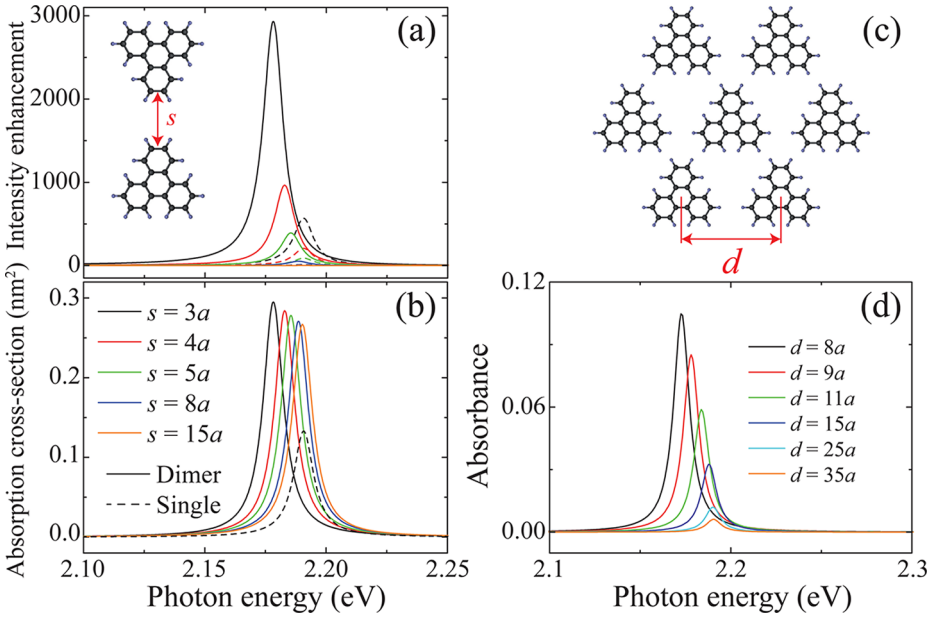

Figure 6. Plasmonic interaction between molecules. (a,b) Field enhancement at the gap center and absorption cross-section for a dimer of triphenylene molecules arranged in a bowtie configuration (see inset in panel a). Different values of the carbon-to-carbon spacing *s* between the two molecules are considered, expressed in units of the C−C bond distance, *a* = 0.142 nm. (c,d). Hexagonal periodic arrangement of triphenylene molecules and plasmonic resonance in the resulting optical absorbance for various values of the lattice constant *d*. These calculations are performed with the TB-RPA method.

strength of the lowest-energy plasmon increases with both molecule length and charge state, while the higher-energy plasmon shows only a mild dependence on these parameters (see Figure 5c). Additionally, the absorption strength is approximately proportional to both *Q* and *N* (see Figure 5c), which is similar to the dependence on length that is observed in metallic nanorods.

These results are consistent with the observed distribution of induced densities associated with these plasmons in linear benzene chains (Figure 5b, insets): the low-energy feature shows a characteristic +/− standing-wave pattern, with induced charges piling up in a smooth distribution along the perimeter of the molecule, just like the classical longitudinal dipole plasmon in metallic nanorods,[38] in which the charge piles up at the particle surface. In contrast, the higher-energy plasmon involves charge pileup in the inner atoms, with oscillations across nearest-neighbor carbons, thus making atomic details conspicuous, and producing charge repulsion that raises the mode energy, which eventually saturates at a finite value for long molecules.

Interaction between PAHs: Toward Molecular Plasmonics and Metamaterials. An attractive possibility opened by molecular plasmonics consists in using PAHs as building blocks that are integrated in larger structures. Graphene-like structures have been recently proposed for a bottom-up approach toward negative refraction based upon a quantum description of the conductivity and a classical treatment of the electrical currents driven by optical fields.[39] In a more general context, the interaction between the plasmons of neighboring molecules defines an atomic-scale approach toward the control of light with an unprecedented degree of spatial confinement. We discuss two prototypical

examples of this idea in Figure 6: dimers and periodic arrays of molecules. For simplicity, we present calculations for relatively small triphenylene molecules using the TB-RPA method. We observe a substantial degree of intermolecule plasmonic interaction, which is remarkable considering the small size of triphenylene. Like in traditional metal-based plasmonics,[38] the interaction between neighboring plasmons results in energy shifts. Because of the relatively small size of the molecules, only the bonding mode (corresponding to parallel polarization) is visible in the far-field spectra, whereas antibonding modes (antiparallel polarization) are dark. The redshift resulting from the attractive interaction between parallel dipoles is moderate for dimers (Figure 6b), clearly becoming larger than the plasmon width for the periodic structures. This is the result of a pure Coulombic interaction between molecules that are not overlapping electronically, as they are separated by carbon-to-carbon distances that are larger than 0.5 nm. The magnitude of the absorbance produced by the arrays (reaching >10%, see Figure 6d) is remarkable considering the small filling fraction of area occupied by the molecules (<20%). The large optical field enhancement in the gap between the molecules (Figure 6a) is equally surprising and suggests the possibility of using molecular plasmons to drive nonlinear response either intrinsically or in molecules decorated with PAHs. By analogy to surface-enhanced Raman scattering (SERS), one can conceive molecular-plasmon-enhanced Raman scattering to trace the presence of other molecules, thus bringing the size of sensing devices down to the atomic scale.

CONCLUSIONS

We have shown that PAHs with armchair edges can sustain optical excitations at visible and near-infrared frequencies and that their energies are strongly dependent on the charge state of the molecules, to the point that the addition or removal of a single electron can switch on/off the existence of such excitations. The mode frequencies are strongly modified when the effect of electron–electron interactions is taken into account either through a TDDFT method or through a simplified TB-RPA approach. This is interpreted as a signature of collective electron motion, either in the form of multiply coupled electron–hole pair excitations or severe renormalization of individual electron–hole pairs due to efficient polarization of other modes. Because of this incipient collective character, and in analogy with graphene plasmons, we refer to these doping-induced optical resonances as molecular plasmons.

The existence of tunable plasmons in molecule-sized graphene structures has to be contrasted with the lack of well-defined plasmons in noble-metal nanoparticles of similar diameter, where nonlocal Landau damping plays a relevant role (*i.e.*, plasmons can directly decay into electron–hole pairs). Additionally, our study poses new questions, such as how many plasmons can be supported by a molecule with a small number of valence electrons, and how large is the nonlinearity arising from the difference between the energy of a two-plasmon state and twice the energy of one plasmon. These nonlinear effects, which are essentially absent from traditional metallic nanoparticles, could be exploited in nonlinear optical applications.

Other types of unique plasmonic applications of PAH structures include the optical detection of atoms/molecules that act as charge donors or acceptors. Here, new plasmonic features would signal the occurrence of a charge transfer reaction. As already demonstrated for graphene in the infrared,[40,41] electrical doping in a gated device could be used to maintain a certain fraction of molecules deposited on a transparent gate (*e.g.*, ITO) in a charged state, thus enabling light modulation in the visible through fast electrical gating technology. The magnitudes of the absorption cross-sections of the plasmons are comparable with the physical cross-section of the molecules, which could therefore be exploited to produce electrically tunable complete optical absorption[42] (perfect absorbers) in the visible. Finally we note that the plasmon linewidths (which have been fixed to 10 meV in the present calculations to facilitate the visualization of the spectra) are likely to be even narrower in realistic systems. Such sharp plasmons may also provide large field enhancements and be used in plasmonic waveguide applications.

PAH molecules can be regarded as nanometer-sized fragments of graphene, but exhibit plasmons in the visible rather than in the mid infrared part of the spectrum. The availability of chemical methods for the synthesis of these molecules makes it possible to generate defect-free identical structures. An interesting aspect of the molecular plasmons under investigation is that they require quantum mechanics to be properly described, and the interaction with each individual electron of the molecules is important. Although the TDDFT method here employed provides an efficient and reasonably accurate tool to describe many-electron quantum interactions, we also demonstrate that the simpler and more computationally affordable TB-RPA method provides a semiquantitative description even for the smallest molecules under consideration. We believe that our study paves the way for a new area in nanophotonics benefiting from the unique plasmonic properties of molecular plasmons.

METHODS

DFT and TDDFT simulations. Ground state density-functional theory (DFT) calculations are performed using the SIESTA method.[43] We use the local-density approximation (LDA)[44] to the exchange and correlation energy and a double-ζ polarized (DZP) basis set. This yields nearly identical results compared

with the generalized gradient approximation (GGA).[45] The DZP basis contains 13 orbitals per C atom and 5 orbitals per H atom. The radii of those orbitals are determined by an energy shift of 100 meV,[43] and the fineness of the real-space mesh is equivalent to a plane-wave cutoff of 100 Ry. We take all PAH atomic structures to be planar, with C−C and C−H distances of 0.142 and 0.109 nm, respectively. In the structural optimizations discussed in the SI, we consider that the molecules are relaxed when all force components are smaller than 0.4 eV/nm. Kohn−Sham orbitals and energies obtained with SIESTA are taken as input to calculate the optical response of the system within TDDFT,[46] using a recently developed fast iterative method.[47,48] We disregard spin-polarization effects, which we find to produce marginal energy shifts in the electronic energies, and therefore, we expect them to contribute negligibly to the optical response.

TB-RPA Simulations. We formulate a tight-binding Hamiltonian using similar methods as for graphene,[49,50] with each atom contributing with one p_z orbital oriented perpendicularly to the plane of the carbons (the local plane in the case of C_{60}), and a hopping energy $t = 2.8$ eV connecting nearest neighbors. Upon diagonalization, we obtain one-electron states that are filled up depending on the charge state of the molecule. These states are used to evaluate the RPA susceptibility χ_0, with spin degeneracy simply included through a factor of 2 in χ_0. More details of this method have been given elsewhere.[27]

The intrinsic width of all excitations is fixed to $\hbar\tau = 10$ meV in both the TDDFT and the TB-RPA calculations to phenomenologically represent the effect of inelastic losses.

Conflict of Interest: The authors declare no competing financial interest.

Acknowledgment. This work has been supported in part by the Spanish MICINN (MAT2010-14885, FIS2010-19609-C02-00, and Consolider NanoLight.es), the European Commission (FP7-ICT-2009-4-248909-LIMA and FP7-ICT-2009-4-248855-N4E), and the Etortek program. A.M. acknowledges financial support through FPU from the Spanish MEC. P.K. aknowledges support from the CSIC JAE-doc program, cofinanced by the European Science Foundation. P.N. acknowledges support from the Robert A. Welch Foundation (C-1222) and the Office of Naval Research (N00014-10-1-0989).

Supporting Information Available: We provide additional information on the comparison between TDDFT and TB-RPA, the effect of self-consistent screening in TDDFT, the effect of structural relaxation, plasmon spectra for linear PAHs, and a comparison of TDDFT theory and experiment for a spectrum of C_{60}. This material is available free of charge *via* the Internet at http://pubs.acs.org.

REFERENCES AND NOTES

1. Zia, R.; Schuller, J. A.; Chandran, A.; Brongersma, M. L. Plasmonics: The Next Chip-Scale Technology. *Mater. Today* **2006**, *9*, 20–27.
2. Engheta, N. Circuits with Light at Nanoscales: Optical Nanocircuits Inspired by Metamaterials. *Science* **2007**, *317*, 1698–1702.
3. Bozhevolnyi, S. I.; Volkov, V. S.; Devaux, E.; Laluet, J. Y.; Ebbesen, T. W. Channel Plasmon Subwavelength Waveguide Components Including Interferometers and Ring Resonators. *Nature* **2006**, *440*, 508–511.
4. Manjavacas, A.; García de Abajo, F. J. Robust Plasmon Waveguides in Strongly Interacting Nanowire Arrays. *Nano Lett.* **2009**, *9*, 1285–1289.
5. Li, K. R.; Stockman, M. I.; Bergman, D. J. Self-Similar Chain of Metal Nanospheres as an Efficient Nanolens. *Phys. Rev. Lett.* **2003**, *91*, 227402.
6. Polman, A. Plasmonics Applied. *Science* **2008**, *322*, 868–869.
7. Stockman, M. I. Nanoplasmonics: The Physics behind the Applications. *Phys. Today* **2011**, *February*, 39–44.
8. Grzelczak, M.; Pérez-Juste, J.; Mulvaney, P.; Liz-Marzán, L. M. Shape Control in Gold Nanoparticle Synthesis. *Chem. Soc. Rev.* **2008**, *37*, 1783–1791.
9. Pileni, M. P. Control of the Size and Shape of Inorganic Nanocrystals at Various Scales from Nano to Macrodomains. *J. Phys. Chem. C* **2007**, *111*, 9019–9038.
10. Kuzyk, A.; Schreiber, R.; Fan, Z.; Pardatscher, G.; Roller, E.-M.; Högele, A.; Simmel, F. C.; Govorov, A. O.; Liedl, T. DNA-Based Self-Assembly of Chiral Plasmonic Nanostructures with Tailored Optical Response. *Nature* **2012**, *483*, 311–314.
11. Shen, J.; Zhu, Y.; Yang, X.; Li, C. Graphene Quantum Dots: Emergent Nanolights for Bioimaging, Sensors, Catalysis and Photovoltaic Devices. *Chem. Commun.* **2012**, *48*, 3686–3699.
12. Roncali, J. Synthetic Principles for Bandgap Control in Linear π-Conjugated Systems. *Chem. Rev.* **1997**, *97*, 173–205.
13. Wu, J.; Pisula, W.; Müllen, K. Graphenes as Potential Material for Electronics. *Chem. Rev.* **2007**, *107*, 718–747.
14. Feng, X.; Liu, M.; Pisula, W.; Takase, M.; Li, J.; Müllen, K. Supramolecular Organization and Photovoltaics of Triangle-Shaped Discotic Graphenes with Swallow-Tailed Alkyl Substituents. *Adv. Mater.* **2008**, *20*, 2684–2689.
15. Feng, X.; Pisula, W.; Müllen, K. Large Polycyclic Aromatic Hydrocarbons: Synthesis and Discotic Organization. *Pure Appl. Chem.* **2009**, *81*, 2203–2224.
16. Rieger, R.; Müllen, K. Forever Young: Polycyclic Aromatic Hydrocarbons as Model Cases for Structural and Optical Studies. *J. Phys. Org. Chem.* **2010**, *23*, 315–325.
17. McKay, D. S.; Gibson, E. K.; Thomas-Keprta, K. L.; Vali, H.; Romanek, C. S.; Clemett, S. J.; Maechling, X. D. F. C. C. R.; Zare, R. N. Search for Past Life on Mars: Possible Relic Biogenic Activity in Martian Meteorite ALH84001. *Science* **1996**, *273*, 924–930.
18. Zhang, K.; Guo, B.; Colarusso, P.; Bernath, P. F. Far-Infrared Emission Spectra of Selected Gas-Phase PAHs: Spectroscopic Fingerprints. *Science* **1996**, *274*, 582–583.
19. Malloci, G.; Mulas, G.; Cappellini, G.; Joblin, C. Time-Dependent Density Functional Study of the Electronic Spectra of Oligoacenes in the Charge States −1, 0, +1, and +2. *Chem. Phys.* **2007**, *340*, 43–58.
20. Malloci, G.; Cappellini, G.; Mulas, G.; Mattoni, A. Electronic and Optical Properties of Families of Polycyclic Aromatic Hydrocarbons: A Systematic (Time-Dependent) Density Functional Theory Study. *Chem. Phys.* **2011**, *384*, 19–27.
21. Chen, J.; Badioli, M.; Alonso-González, P.; Thongrattanasiri, S.; Huth, F.; Osmond, J.; Spasenović, M.; Centeno, A.; Pesquera, A.; Godignon, P.; *et al.* Optical Nano-Imaging of Gate-Tunable Graphene Plasmons. *Nature* **2012**, *487*, 77–81.
22. Fei, Z.; Rodin, A. S.; Andreev, G. O.; Bao, W.; McLeod, A. S.; Wagner, M.; Zhang, L. M.; Zhao, Z.; Thiemens, M.; Dominguez, G.; *et al.* Gate-Tuning of Graphene Plasmons Revealed by Infrared Nano-Imaging. *Nature* **2012**, *487*, 82–85.
23. Nagao, T.; Yaginuma, S.; Inaoka, T.; Sakurai, T. One-Dimensional Plasmon in an Atomic-Scale Metal Wire. *Phys. Rev. Lett.* **2006**, *97*, 116802.
24. Keller, J. W.; Coplan, M. A. Electron Energy Loss Spectroscopy of C_{60}. *Chem. Phys. Lett.* **1992**, *193*, 89–92.
25. Stéphan, O.; Taverna, D.; Kociak, M.; Suenaga, K.; Henrard, L.; Colliex, C. Dielectric Response of Isolated Carbon Nanotubes Investigated by Spatially Resolved Electron Energy-Loss Spectroscopy: From Multiwalled to Single-Walled Nanotubes. *Phys. Rev. B* **2002**, *66*, 155422.
26. Jablan, M.; Buljan, H.; Soljačić, M. Plasmonics in Graphene at Infrared Frequencies. *Phys. Rev. B* **2009**, *80*, 245435.
27. Thongrattanasiri, S.; Manjavacas, A.; García de Abajo, F. J. Quantum Finite-Size Effects in Graphene Plasmons. *ACS Nano* **2012**, *6*, 1766–1775.
28. Koppens, F. H. L.; Chang, D. E.; García de Abajo, F. J. Graphene Plasmonics: A Platform for Strong Light-Matter Interactions. *Nano Lett.* **2011**, *11*, 3370–3377.
29. Fernández-Rossier, J.; Palacios, J. J. Magnetism in Graphene Nanoislands. *Phys. Rev. Lett.* **2007**, *99*, 177204.
30. Kobayashi, Y.; Fukui, K.; Enoki, T.; Kusakabe, K.; Kaburagi, Y. Observation of Zigzag and Armchair Edges of Graphite Using Scanning Tunneling Microscopy and Spectroscopy. *Phys. Rev. B* **2005**, *71*, 193406.

31. Christensen, J.; Manjavacas, A.; Thongrattanasiri, S.; Koppens, F. H. L.; García de Abajo, F. J. Graphene Plasmon Waveguiding and Hybridization in Individual and Paired Nanoribbons. *ACS Nano* **2012**, *6*, 431–440.
32. Liebsch, A. Surface-Plasmon Dispersion and Size Dependence of Mie Resonance: Silver *versus* Simple Metals. *Phys. Rev. B* **1993**, *48*, 11317–11328.
33. Bernadotte, S.; Evers, F.; Jacob, C. R. Plasmons in Molecules. *J. Phys. Chem. C* **2013**, *117*, 1863–1878.
34. Pines, D.; Nozières, P. *The Theory of Quantum Liquids*; W. A. Benjamin, Inc.: New York, 1966.
35. Kivelson, S.; Chapman, O. L. Polyacene and a New Class of Quasi-One-Dimensional Conductors. *Phys. Rev. B* **1983**, *28*, 7236–7243.
36. Bettinger, H. F. Electronic Structure of Higher Acenes and Polyacene: The Perspective Developed by Theoretical Analyses. *Pure Appl. Chem.* **2010**, *82*, 905–915.
37. Novotny, L. Effective Wavelength Scaling for Optical Antennas. *Phys. Rev. Lett.* **2007**, *98*, 266802.
38. Myroshnychenko, V.; Rodríguez-Fernández, J.; Pastoriza-Santos, I.; Funston, A. M.; Novo, C.; Mulvaney, P.; Liz-Marzán, L. M.; García de Abajo, F. J. Modelling the Optical Response of Gold Nanoparticles. *Chem. Soc. Rev.* **2008**, *37*, 1792–1805.
39. Sha, X. W.; Economou, E. N.; Papaconstantopoulos, D. A.; Pederson, M. R.; Mehl, M. J.; Kafesaki, M. Possible Molecular Bottom-Up Approach to Optical Metamaterials. *Phys. Rev. B* **2012**, *86*, 115404.
40. Chen, C. F.; Park, C. H.; Boudouris, B. W.; Horng, J.; Geng, B.; Girit, C.; Zettl, A.; Crommie, M. F.; Segalman, R. A.; Louie, S. G.; *et al*. Controlling Inelastic Light Scattering Quantum Pathways in Graphene. *Nature* **2011**, *471*, 617–620.
41. Fang, Z.; Thongrattanasiri, S.; Schlather, A.; Liu, Z.; Ma, L.; Wang, Y.; Ajayan, P. M.; Nordlander, P.; Halas, N. J.; García de Abajo, F. J. Gated Tunability and Hybridization of Localized Plasmons in Nanostructured Graphene. *ACS Nano* **2013**, *7*, 2388–2395.
42. Thongrattanasiri, S.; Koppens, F. H. L.; García de Abajo, F. J. Complete Optical Absorption in Periodically Patterned Graphene. *Phys. Rev. Lett.* **2012**, *108*, 047401.
43. Soler, J. M.; Artacho, E.; Gale, J. D.; García, A.; Junquera, J.; Ordejón, P.; Sánchez-Portal, D. The SIESTA Method for *ab initio* Order-N Materials Simulations. *J. Phys.: Condens. Matter* **2002**, *14*, 2745–2779.
44. Perdew, J. P.; Zunger, A. Self-Interaction Correction to Density-Functional Approximations for Many-Electron Systems. *Phys. Rev. B* **1981**, *23*, 5048–5079.
45. Varsano, D.; Di Felice, R.; Marques, M. A. L.; Rubio, A. A TDDFT Study of the Excited States of DNA Bases and their Assemblies. *J. Phys. Chem. B* **2006**, *110*, 7129–7138.
46. Marques, M. A. L.; Ullrich, C. A.; Nogueira, F.; Rubio, A.; Burke, K.; Gross, E. K. U. *Time-Dependent Density Functional Theory*; Springer: Berlin, 2006; Vol. 706.
47. Koval, P.; Foerster, D.; Coulaud, O. A Parallel Iterative Method for Computing Absorption Spectra. *J. Chem. Theor. Comput.* **2010**, *6*, 2654–2668.
48. Koval, P.; Foerster, D.; Coulaud, O. Fast Construction of the Kohn−Sham Response Function for Molecules. *Phys. Status Solidi* **2010**, *247*, 1841–1848.
49. Wallace, P. R. The Band Theory of Graphite. *Phys. Rev.* **1947**, *71*, 622–634.
50. Castro Neto, A. H.; Guinea, F.; Peres, N. M. R.; Novoselov, K. S.; Geim, A. K. The Electronic Properties of Graphene. *Rev. Mod. Phys.* **2009**, *81*, 109–162.